

Proceedings of the International Symposium on Physics of Materials (ISPMA 14), September 10–15, 2017, Prague

Nanotwinning and Modulation of Martensitic Structures in Ni_2MnGa Alloy: An *ab initio* Study

M. ZELENÝ*

Institute of Materials Science and Engineering, NETME Centre, Faculty of Mechanical Engineering, Brno University of Technology, Technická 2896/2, CZ-61669 Brno, Czech Republic

The *ab initio* electronic structure calculations show importance of nanotwinning concept for understanding martensitic lattice geometry in Ni_2MnGa magnetic shape memory alloys. All modulated martensitic structures, 4O, 10M and 14M, are stabilized due to the presence of nanotwin double layers in the structure, i.e., nanotwins consisting of two (101) lattice planes of nonmodulated martensitic structure. In all structures, the most significant decrease of total energy arises from a shift of Mn and Ga atoms at the nanotwin boundaries by about 1% of atomic coordinate.

DOI: [10.12693/APhysPolA.134.658](https://doi.org/10.12693/APhysPolA.134.658)

PACS/topics: 62.20.fg, 31.15.es, 61.66.–f

1. Introduction

The Ni–Mn–Ga alloys belong to the class of magnetic shape memory (MSM) materials, which hold a large potential for a wide range of applications including actuators, sensors, energy harvesters, and even magnetic refrigeration systems [1–4]. The most studied phenomenon exhibited by the MSM alloys is a giant magnetic field-induced strain (MFIS) [5] that can reach up to 12% [6]. The MFIS occurs by the rearrangement of twins in an applied external magnetic field [5] and its magnitude primarily depends on martensite microstructure [7–9].

At elevated temperature, there is a single austenitic phase of Ni–Mn–Ga with cubic $L2_1$ structure. Several martensitic phases have been observed below the martensitic transformation temperature, which occurs at 202 K for stoichiometric Ni_2MnGa [10] and further changes for off-stoichiometric alloys [11, 12]. Some martensitic structures with $c/a < 1$ exhibit modulation of (110) planes in the $[1\bar{1}0]$ direction with a periodicity of 5 or 7 lattice planes (denoted as 10M or 14M). The 10M martensite observed for near stoichiometric composition [10, 11] exhibits a MFIS of about 6% [7] and its structure is almost tetragonal with very small monoclinic angle and a/b ratio close to 1 [7, 8]. The monoclinic 14M martensite has been reported for compositions far from stoichiometry exhibiting a MFIS of about 10% [9]. A MFIS of 12% has been reported in NM martensite of Ni–Mn–Ga doped by Co and Cu, which has a tetragonally distorted $L2_1$ lattice with $c/a = 1.14$ and does not exhibit modulation [6]. NM martensite with $c/a = 1.21$ is also stable in significantly off-stoichiometric Ni–Mn–Ga [11, 12]; however, it shows no MFIS. Moreover, for certain alloy compositions the (10M \rightarrow)14M \rightarrow NM sequence of intermartensitic transformations occurs with decrease of temperature [13, 14] or by applying external stress [15, 16].

Using the nanotwinning concept [17] the modulated structures can be described by a monoclinic lattice with an alternating sequence of nanotwins constituted from (101) lattice planes of NM structure as basal planes [18, 19]. A structure with the width of five lattice planes in one orientation and the width of two planes in opposite orientation (denoted as $(5\bar{2})_2$ in the Zhdanov notation [20]) describes 14M structure. The $(5\bar{2})_2$ is repeated twice to fulfill the periodicity of atomic ordering (Fig. 1a). Similarly, 10M structure (Fig. 1b) can be considered as alternating nanotwins of width three and two lattice planes (denoted as $(3\bar{2})_2$). In contrast to orthorhombic structures with harmonic modulation [21, 22], the fully relaxed $(3\bar{2})_2$ and $(5\bar{2})_2$ structures with nanotwins give *ab initio* total energies very close to the total energy of the NM structure [23, 24]. Thus, the nanotwinning description provides better agreement with the experimental observation of 10M structure as a ground state in stoichiometric Ni_2MnGa , although the NM martensite still exhibits lower energy.

Existence of nanotwins made up of two (101) lattice planes in both structures indicates that this nanotwin double layer could be the most prominent building block of modulated structure. Our recent *ab initio* calculations [25] confirmed the importance of nanotwin double layer for stabilization of modulated structures, because the $(2\bar{2})_1$ structure constituted only from oppositely oriented nanotwin double layers (Fig. 1c), denoted also as 4O, exhibits the total energy approximately about 2 meV/atom lower than other martensites. This newly predicted structure has orthorhombic symmetry with the modulation periodicity of four lattice planes.

Nanotwins in NM martensite created by pure geometrical construction [19] does not provide structures with the lowest total energies. These artificially constructed ideal structures are further stabilized within the relaxation process by small changes of lattice parameters and atomic positions. The most essential decrease of the total energy in 4O structure arises from the shift of Mn and Ga atoms in x direction at the nanotwin bound-

*e-mail: zeleny@fme.vutbr.cz

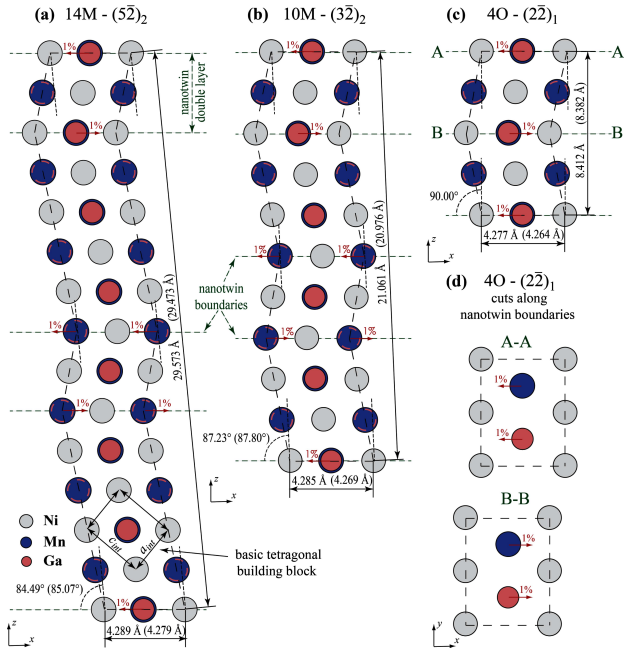


Fig. 1. Fully relaxed crystal structures of 14M (a), 10M (b) and 4O (c) martensites described by nanotwinning concept and cuts of 4O structure along the nanotwin boundaries (d). Lattice parameters of fully relaxed structures are marked (lattice parameters of ideal structures with minimized $(c/a)_{int}$ before relaxation are in parentheses). Green dashed lines indicate nanotwin boundaries. The shifts of Mn and Ga atoms in x direction responsible for significant decrease of total energy are marked by red arrows. Red dashed circles mark Ga atoms in the atomic layer underneath the figure plane.

aries within the double layer approximately about 1% of atomic coordinate (Fig. 1d) as was shown in our previous work [25]. The purpose of this work is to provide similar detailed description of relaxation processes for experimentally observed 10M and 14M structures described by nanotwinning concept. Our *ab initio* calculations will clearly demonstrate the importance of nanotwin double layer for the stability of all modulated structures.

2. Computational details

The *ab initio* calculations were performed using the Vienna Ab initio Simulation Package (VASP) [26, 27] in which the electron-ion interaction was described by projector augmented-wave potentials [28, 29]. The electronic orbitals were expanded in terms of plane waves with a maximum kinetic energy of 600 eV. We used the gradient-corrected exchange-correlation functional proposed by Perdew, Burke, and Ernzerhof [30]. The Brillouin zone (BZ) was sampled using a Γ -point-centered mesh with the smallest allowed spacing between k -points equal to 0.1 \AA^{-1} in each direction of the reciprocal lattice vectors. This setting ensured constant k -point density in all our calculations. The integration over the BZ used the Methfessel-Paxton smearing method [31] with a 0.02 eV smearing width. Settings for k -point density and

smearing width were obtained with the help of an adaptive smearing method [32]. The total energy was calculated with high precision by convergence to 10^{-7} eV per computational cell. Relaxation of the atomic positions and structural parameters was performed with the quasi-Newton algorithm, using the exact Hellmann-Feynman forces, and was considered to be converged after all forces dropped below 1 meV/\AA .

In purely geometrical construction of ideal nanotwinned structures, there are only two independent parameters: cell volume and internal $(c/a)_{int}$ of basic tetragonal building blocks [19] (see Fig. 1a). These building blocks correspond to one eighths of $L2_1$ lattice for $(c/a)_{int} = 1$ or NM lattice for $(c/a)_{int} = 1.2503$, which is the calculated equilibrium $(c/a)_{NM}$ ratio. Compared to experimental value of $(c/a)_{NM} = 1.21$, the calculated value is overestimated, which is usual for *ab initio* calculations [21, 23, 33]. The volume was kept constant at $194.63 \text{ \AA}^3/\text{atom}$ for ideal structures, because there are only small volume differences between martensites. Other lattice parameters and atomic positions of ideal structures can be further derived according to equations in Ref. [19].

Although the unconstrained relaxation leads directly to structures with the lowest total energy, we artificially divided the relaxation process into three constrained steps to estimate their contributions to total energies: (a) searching for equilibrium $(c/a)_{int}$, (b) relaxation of Mn and Ga atoms in nanotwin boundaries in x direction and (c) relaxation of lattice parameters. Contrary to our previous work [25] we performed the relaxation of Mn and Ga atoms before the relaxation of lattice parameters, because the shift of Mn and Ga atoms has stronger influence on total energy.

3. Results

All ideal nanotwinned structures with $(c/a)_{int} = (c/a)_{NM}$ exhibit total energies higher than NM martensite. The difference is approximately 1 meV/atom for 4O and 14M martensite and 2.5 meV/atom for 10M (compare energies on vertical line in Fig. 2a). The total energy can be further decreased by finding of the equilibrium $(c/a)_{int}$. All structures corresponding to displayed energies in Fig. 2a can be considered as ideal, because they fulfil the definitions in Ref. [19]. Lattice parameters of ideal structures with the equilibrium $(c/a)_{int}$ can be found in Fig. 1 in parentheses. For 14M martensite the energy minimum lies at $(c/a)_{int} = 1.2214$, where the total energy decreases by about 0.4 meV/atom . The effect of relaxation is stronger for 10M martensite, because the minimum corresponds to $(c/a)_{int} = 1.2108$ and energy decreases by about 0.6 meV/atom . However, the energy is still higher than the energy of 10M martensite described by harmonic modulation (red horizontal dashed line) constructed according to Ref. [21]. Thus, 10M and 14M martensite still exhibit higher energies than the energy of NM structure. The strongest relaxation effect can be found for 4O structure, where

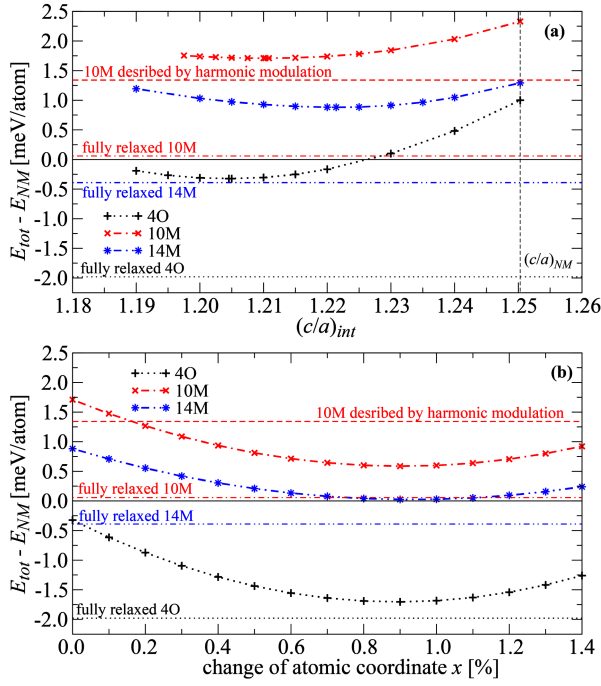


Fig. 2. Total energies with respect to the energy of NM structure as functions of internal $(c/a)_{int}$ (a) and change of atom coordinate of Mn and Ga atoms at the nanotwin boundaries in x direction (b). Black vertical line in (a) corresponds to the equilibrium $(c/a)_{NM}$ of NM structure. Red horizontal lines indicate energies of 10M structure described by harmonic modulation (dashed line) and fully relaxed 10M structure described by nanotwinning concept (dash-and-dot line). Blue horizontal line indicates the energy of fully relaxed 14M structure and black dotted horizontal line corresponds to the energy of fully relaxed 4O structure.

equilibrium $(c/a)_{int} = 1.2045$ and total energy is about 0.3 meV/atom smaller than the energy of NM structure. It corresponds to energy decrease by about 1.3 meV/atom compared to the 4O structure with $(c/a)_{int} = (c/a)_{NM}$.

Differences in equilibrium $(c/a)_{int}$ can be understood as a result of competition between the smallest $(c/a)_{int}$ of nanotwin double layer and the largest $(c/a)_{NM}$ of NM structure. The 4O structure is constituted only by double layers, thus it exhibits the smallest $(c/a)_{int}$. The ratio further increases together with increase of number of layers separating the double layers in 10M martensite (3 layers) and 14M martensite (5 layers). Also the energy gain from minimizing of $(c/a)_{int}$ corresponds to the increasing density of double layers in the structures. The energy gain is more than twice larger in 4O structure, because it also contains twice larger number of double layers than 10M and 14M structures.

Figure 2b) shows how the shift of Mn and Ga atoms in x direction at the nanotwin boundaries further decreases the total energy of structure with equilibrium $(c/a)_{int}$. Although the ideality of the structures is now lost, the overall lattice parameters do not change in this relaxation step and they still correspond to the values obtained ac-

ording to Ref. [19]. The minima for all modulated structures can be found for shift by about 0.9% of atomic coordinate, which corresponds approximately to 0.039 Å. It indicates that the shift is not affected by martensitic structure and originates solely from the geometry of double layer. The energy benefit is the largest again in 4O martensite due to the highest density of double layers and corresponds to 1.38 meV/atom. Thus, the energy of 4O structure lies now 1.70 meV/atom below the energy of NM structure. The shift of Mn and Ga in 10M martensite results in total energy decrease of about 1.12 meV/atom. The 10M structure described by nanotwinning is now preferred by about 0.75 meV/atom compared to 10M structure described by harmonic modulation, but it still lies about 0.59 meV/atom above NM structure. The smallest effect can be seen for 14M structure, where total energy decreases by only about 0.86 meV/atom. Thus, the total energy still remains slightly above the energy of NM structure. As a result of the shift of atoms at nanotwin boundaries, the $(c/a)_{int}$ slightly changes in basic building blocks within nanotwin double layer in Mn–Ga sublattice and these building blocks are not tetragonal anymore but exhibit very small monoclinic distortion.

The last relaxation step comprises full optimization of lattice parameters and remaining atomic positions, which results in complete loss of ideal geometry and small change of volume. The differences between $(c/a)_{int}$ ratios of Ni and Mn–Ga sublattices are now more pronounced as well as the differences between $(c/a)_{int}$ ratio inside and outside of the nanotwin double layers. Basic building blocks are no more tetragonal in whole lattice although their monoclinic distortion is very small, less than 1° . Lattice parameters of fully relaxed and ideal structures can be found in Fig. 1. Obtained contributions to total energies are not as large as in previous relaxation steps. The smallest effect can be found for 4O structure, where energy decreases by about 0.28 meV/atom. Because the structure constitutes only from double layers, almost optimal geometry of the lattice was already achieved in previous steps. The total energy of 14M martensite decreases by about 0.41 meV/atom, which makes 14M structure finally more energetically favorable than NM structure. Full relaxation of 10M structure results in further decrease of the total energy about by 0.53 meV/atom, thus the energy is now just about 0.06 meV/atom higher than the energy of NM structure. The largest energy gain obtained from full relaxation of 10M martensite compared to other modulated structures shows that the pure geometrical construction of ideal nanotwinned structure does not provide very good agreement with the fully relaxed 10M structure. However, the nanotwinning concept is still the best model, which provides a good starting point for obtaining the crystal structure of 10M martensite exhibiting the lowest energy.

4. Conclusions

The *ab initio* calculations were used for investigation of lattice relaxations responsible for stabilization of modulated structures 4O, 10M, and 14M in stoichiometric

Ni₂MnGa martensite. The purely geometrical constructions of modulated lattices based on nanotwinning concept are used as a starting point. Minimizing of $(c/a)_{int}$ at constant volume shows that this single independent parameter of the structures increases in sequence 4O→10M→14M with increasing number of basal planes separating the nanotwin double layers presented in all modulated structures. Compared to fully relaxed structures, the geometrically constructed ideal structures exhibit significantly higher energies. Only the energy of 4O structure lies below the energy NM structure, which exhibits the biggest $(c/a)_{int}$ ratio and contains no nanotwins. Total energies of modulated structures can be further significantly lowered by the shift of Mn and Ga atoms in x direction at the nanotwin boundaries by about 0.9% of atomic coordinate. The energy gain from this shift for 10M and 14M structures is not as big as for 4O structure. However, it is still the most beneficial step of relaxation process. Because the shift is almost the same in all modulated structures, this lattice distortion originates only in presence of nanotwin double layer and it does not depend on overall geometry of the structure. It confirms the importance of nanotwin double layers for the stabilization of all modulated structures. Further full optimization of lattice parameters and atomic positions pushes the lattices far away from its initial (ideal) geometry. Although this step has less significant effect on the total energies of 10M and 14M structures than the previous one, the total energies finally reach the same level as energy of NM structure.

Acknowledgments

This research was supported by the Ministry of Education, Youth and Sports of the Czech Republic within the support program “National Sustainability Programme I” (Project NETME CENTRE PLUS-LO1202).

References

- [1] M. Acet, L. Mañosa, A. Planes, in: *Handbook of Magnetic Materials*, Ed. K.H.J. Buschow, Vol. 19, Elsevier, Amsterdam 2011, p. 231.
- [2] O. Heczko, N. Scheerbaum, O. Gutfleisch, in: *Nanoscale Magnetic Materials and Applications*, Eds. J. Liu, E. Fullerton, O. Gutfleisch, D. Sellmyer, Springer, Berlin 2009, p. 339.
- [3] S.A. Wilson, R.P.J. Jourdain, Q. Zhang, R.A. Dorey, C.R. Bowen, M. Willander, Q. Wahab, M. Willander, S.M. Al-hilli, O. Nur, E. Quandt, C. Johansson, E. Pagounis, M. Kohl, J. Matovic, B. Samel, W. van der Wijngaart, E.W.H. Jager, D. Carlsson, Z. Djinovic, M. Wegener, C. Moldovan, R. Iosub, E. Abad, M. Wendlandt, C. Rusu, K. Persson, *Mater. Sci. Eng. R Rep.* **56**, 1 (2007).
- [4] V.V. Khovaylo, V.V. Rodionova, S.N. Shevyrtalov, V. Novosad, *Phys. Status Solidi B* **251**, 2104 (2014).
- [5] K. Ullakko, J.K. Huang, C. Kantner, R.C. O’Handley, V.V. Kokorin, *Appl. Phys. Lett.* **69**, 1966 (1996).
- [6] A. Sozinov, N. Lanska, A. Soroka, W. Zou, *Appl. Phys. Lett.* **102**, 021902 (2013).
- [7] S.J. Murray, M.A. Marioni, S.M. Allen, R.C. O’Handley, T.A. Lograsso, *Appl. Phys. Lett.* **77**, 886 (2000).
- [8] O. Heczko, A. Sozinov, K. Ullakko, *IEEE Trans. Magn.* **36**, 3266 (2000).
- [9] A. Sozinov, A.A. Likhachev, N. Lanska, K. Ullakko, *Appl. Phys. Lett.* **80**, 1746 (2002).
- [10] P.J. Webster, K.R.A. Ziebeck, S.L. Town, M.S. Peak, *Philos. Mag. B* **49**, 295 (1984).
- [11] N. Lanska, O. Söderberg, A. Sozinov, Y. Ge, K. Ullakko, V.K. Lindroos, *J. Appl. Phys.* **95**, 8074 (2004).
- [12] A. Çakır, L. Righi, F. Albertini, M. Acet, M. Farle, S. Aktürk, *J. Appl. Phys.* **114**, 183912 (2013).
- [13] C. Seguí, V.A. Chernenko, J. Pons, E. Cesari, V. Khovailo, T. Takagi, *Acta Mater.* **53**, 111 (2005).
- [14] L. Straka, O. Heczko, N. Lanska, *IEEE Trans. Magn.* **38**, 2835 (2002).
- [15] V.V. Martynov, V.V. Kokorin, *J. Phys. III* **2**, 739 (1992).
- [16] Y. Ge, N. Zárubová, O. Heczko, S.-P. Hannula, *Acta Mater.* **90**, 151 (2015).
- [17] M.E. Gruner, R. Niemann, P. Entel, R. Pentcheva, U.K. Röföler, K. Nielsch, S. Fähler, *Sci. Rep.* **8**, 8489 (2018).
- [18] S. Kaufmann, U.K. Röföler, O. Heczko, M. Wuttig, J. Buschbeck, L. Schultz, S. Fähler, *Phys. Rev. Lett.* **104**, 145702 (2010).
- [19] R. Niemann, S. Fähler, *J. Alloys Comp.* **703**, 280 (2017).
- [20] G.S. Zhdanov, *Compt. Rend. Acad. Sci. USSR* **48**, 39 (1945).
- [21] A.T. Zayak, P. Entel, J. Enkovaara, A. Ayuela, R.M. Nieminen, *J. Phys. Condens. Matter* **15**, 159 (2003).
- [22] N. Xu, J.-M. Raulot, Z.-B. Li, J. Bai, Y.-D. Zhang, X. Zhao, L. Zuo, C. Esling, *Appl. Phys. Lett.* **100**, 084106 (2012).
- [23] R. Niemann, U.K. Röföler, M.E. Gruner, L. Schultz, S. Fähler, *Adv. Eng. Mater.* **14**, 562 (2012).
- [24] B. Dutta, A. Çakır, C. Giacobbe, A. Al-Zubi, T. Hickel, M. Acet, J. Neugebauer, *Phys. Rev. Lett.* **116**, 025503 (2016).
- [25] M. Zelený, L. Straka, A. Sozinov, O. Heczko, *Phys. Rev. B* **94**, 224108 (2016).
- [26] G. Kresse, J. Furthmüller, *Phys. Rev. B* **54**, 11169 (1996).
- [27] G. Kresse, J. Furthmüller, *Comput. Mater. Sci.* **6**, 15 (1996).
- [28] P.E. Blöchl, *Phys. Rev. B* **50**, 17953 (1994).
- [29] G. Kresse, D. Joubert, *Phys. Rev. B* **59**, 1758 (1999).
- [30] J.P. Perdew, K. Burke, M. Ernzerhof, *Phys. Rev. Lett.* **77**, 3865 (1996); *ibid.*, **78**, 1396(E) (1997).
- [31] M. Methfessel, A.T. Paxton, *Phys. Rev. B* **40**, 3616 (1989).
- [32] T. Björkman, O. Grånäs, *Int. J. Quantum Chem.* **111**, 1025 (2011).
- [33] A. Ayuela, J. Enkovaara, R.M. Nieminen, *J. Phys. Condens. Matter* **14**, 5325 (2002).